

WISE J061213.85-303612.5: a new T-dwarf binary candidate[★], ^{★★}

N. Huélamo¹, V. D. Ivanov^{2,3}, R. Kurtev^{4,5}, J. H. Girard², J. Borissova^{4,5}, D. Mawet², K. Mužić², C. Cáceres⁴, C. H. F. Melo², M. F. Sterzik³, and D. Minniti^{5,6}

¹ Centro de Astrobiología (INTA-CSIC); ESAC Campus, P.O. Box 78, E-28691 Villanueva de la Cañada, Spain
e-mail: nhuelamo@cab.inta-csic.es

² European Southern Observatory, Alonso de Cordova 3107, Casilla 19, Vitacura, Santiago, Chile

³ European Southern Observatory, Karl Schwarzschild Strasse 2, Garching bei München, D-85748 Germany

⁴ Instituto de Física y Astronomía, Universidad de Valparaíso, Av. Gran Bretaña 1111, 2360102, Valparaíso, Chile

⁵ Milenium Institute of Astrophysics, MAS

⁶ Departamento de Ciencias Físicas, Universidad Andrés Bello, República 220, 837-0134, Santiago, Chile

Received December 31, 2014; accepted —, —

ABSTRACT

Context. T and Y-dwarfs are among the coolest and least luminous objects detected, and they can help to understand the properties of giant planets. Up to now, there are more than 350 T dwarfs that have been identified thanks to large imaging surveys in the infrared, and their multiplicity properties can shed light on the formation process.

Aims. The aim of this work is to look for companions around a sample of seven ultracool objects. Most of them have been discovered by the WISE observatory and have not been studied before for multiplicity.

Methods. We observed a sample six T dwarfs and one L9 dwarf with the Laser Guide Star (LGS) and NAOS-CONICA, the adaptive optics (AO) facility, and the near infrared camera at the ESO Very Large Telescope. We observed all the objects in one or more near-IR filters (JHK_s).

Results. From the seven observed objects, we have identified a subarcsecond binary system, WISE J0612-3036, composed of two similar components with spectral types of T6. We measure a separation of $\rho = 350 \pm 5$ mas and a position angle of $PA = 235 \pm 1^\circ$. Using the mean absolute magnitudes of T6 dwarfs in the 2MASS JHK_s bands, we estimate a distance of $d = 31 \pm 6$ pc and derive a projected separation of $\rho \sim 11 \pm 2$ au. Another target, WISE J2255-3118, shows a very faint object at $1''.3$ in the K_s image. The object is marginally detected in H , and we derive a near infrared color of $H - K_s > 0.1$ mag. *HST/WFC3* public archival data reveals that the companion candidate is an extended source. Together with the derived color, this suggests that the source is most probably a background galaxy. The five other sources are apparently single, with $3\text{-}\sigma$ sensitivity limits between $H = 19\text{--}21$ for companions at separations $\geq 0''.5$.

Conclusions. WISE 0612-3036 is probably a new T-dwarf binary composed of two T6 dwarfs. As in the case of other late T-dwarf binaries, it shows a mass ratio close to 1, although its projected separation, ~ 11 au, is larger than the average (~ 5 au). Additional observations are needed to confirm that the system is bound.

Key words. stars: brown dwarfs — stars: binary — techniques: high angular resolution — individual: WISE J061213.85-303612.5, WISE J225540.75-311842.0

1. Introduction

Brown dwarfs (BDs) are the bridge between late-type stars and planetary-mass objects. T dwarfs (with effective temperatures of $T_{\text{eff}} \sim 1500\text{--}500$ K) and Y-dwarfs ($T_{\text{eff}} \leq 500$ K) are among the coolest and least luminous objects detected, and their properties can help us to understand giant extrasolar planets.

In recent years, a significant number of BDs have been identified in wide-field optical and infrared imaging surveys, e.g., the Two Micron All Sky Survey (2MASS, Skrutskie et al. 2006), the DEep Near Infrared Survey (DENIS, Epchtein et al. 1997), or the UKIRT Infrared Deep Sky Survey (UKIDSS, Lawrence et al. 2007). For the coolest objects, deep near-

IR and mid-IR surveys such as the Canada-France Brown Dwarf Survey (CFBDS, Delorme et al. 2008) or the Wide-Field Infrared Survey Explorer (WISE, Wright et al. 2010) have contributed to significantly increasing the number of known T and Y-dwarfs (e.g., Burningham et al. 2010; Albert et al. 2011; Kirkpatrick et al. 2011; Cushing et al. 2011; Kirkpatrick et al. 2012; Tinney et al. 2012; Pinfield et al. 2014a,b). Currently, there are ~ 355 and 15 identified T and Y dwarfs, respectively.¹

Multiplicity is directly related to the stellar and substellar formation process, and it has been studied for different mass regimes. In the case of T dwarfs, several works have focused on studying the companions around these sources (e.g., Burgasser et al. 2003; Bouy et al. 2003; Burgasser et al. 2006; Bouy et al. 2008; Gelino et al. 2011; Liu et al. 2011, 2012). Most of them have benefited from laser guide star (LGS) adaptive optics (AO) assisted observations at large ground-based telescopes or/and the *Hubble Space Telescope* (HST) data in order to achieve the best angular resolution and sensitivity. As a result there are now ~ 14 identified T-dwarf binaries. Most of them

[★] This work used data collected at the VLT under runs 89.C-0494(A,B,C) and 91.C-0501(A,B).

^{★★} Based on observations made with the NASA/ESA Hubble Space Telescope, and obtained from the Hubble Legacy Archive, which is a collaboration between the Space Telescope Science Institute (STScI/NASA), the Space Telescope European Coordinating Facility (ST-ECF/ESA), and the Canadian Astronomy Data Centre (CADC/NRC/CSA).

¹ www.dwarfarchives.org

show very small separations ($\sim 2\text{-}5$ au, Burgasser et al. 2003, 2006; Liu et al. 2011), although there are also wide binaries that have been detected (e.g., WISEJ1711+3500, $\rho = 15 \pm 2$ au, Liu et al. 2012). In a recent work, Aberasturi et al. (2014) have derived a binary fraction of <16 or $<25\%$, depending on the underlying mass ratio distribution.

Motivated by the large number of T and Y dwarfs identified by WISE, we started a program to search for companions to newly discovered BDs in 2012 using high angular resolution LGS AO-assisted observations in the near-IR. Most of the selected targets were T and Y dwarfs identified with WISE and listed in Kirkpatrick et al. (2011). In this paper we present the results from our AO imaging campaigns. In Sections 2 and 3 we described the sample selection, the observations, and the data reduction. In Section 4 we discuss the main results, including the sensitivity limits. The main conclusions are summarized in Section 5.

2. The sample of brown dwarfs.

Our target list was mainly selected from the newly found BDs with WISE, which is a mid-IR satellite launched in 2009 that surveyed the entire sky in four bands: 3.4, 4.6, 12, and $22\ \mu\text{m}$. Finding BDs was a primary science goal of WISE, and the strategy was based on a particular color cut: the methane absorption feature near $3.3\ \mu\text{m}$ made the [3.6]-[4.6] color extremely red (≥ 2 mag), unique among substellar objects.

Kirkpatrick et al. (2011) summarize the first WISE BDs discoveries that included a list of a hundred of detected substellar objects. For our study, we initially selected WISE T and Y dwarfs from this work. We kept only those observable from Paranal Observatory and never studied for multiplicity before (Galino et al. 2011; Liu et al. 2012).

Additional dwarfs were discovered and studied afterwards (Cushing et al. 2011; Gizis et al. 2011; Kirkpatrick et al. 2012), and we included them in our target list. Finally, we also considered several bright targets (mainly previously known L-type and early-T dwarfs) as backups to be observed under bad conditions. One of these targets, 2MASS J1114-2618, was observed by the *HST* in the meantime, and the results were recently presented by Aberasturi et al. (2014). We include it here for comparison. In total, we selected ~ 50 targets for our study.

3. Observations and data reduction

The observations presented here were obtained with NAOS-CONICA (NACO), the AO system and near-IR camera (Lenzen et al. 2003; Rousset et al. 2003) at the Very Large Telescope (VLT). Since most of the targets are too faint to be used as natural guide stars (NGS), we made use of the laser guide star (LGS) facility at the VLT.

To obtain a full AO correction, the LGS facility should be used in combination with a tip-tilt (*tt*) reference star brighter than $V = 17$ mag, located at a maximum separation of $40''$ from the target. In the absence of a *tt* star, the LGS can be used in the so-called ‘seeing enhancer’ (*se*) mode (Girard et al. 2010), that is, LGS-assisted AO observation but without correcting for tip/tilt. Because the low orders of the wavefront corrugations are not corrected, the SE mode provides an image quality intermediate between simple (non-AO) imaging and full LGS closed loop observations. (We refer to the NACO manual for a full descrip-

tion of this mode.² For our observations, we used a *tt* reference star whenever available, and switched to *se* mode otherwise.

The observations were allocated in seven different nights over 2012 and 2013. We could not collect any data in four of the nights (2012-06-10, 2012-07-12, 2012-12-08, and 2013-03-07) because of inadequate atmospheric conditions for AO and the LGS and/or technical issues associated to the laser itself. The atmospheric conditions in the three other nights were moderate to poor for the LGS, with average coherence times (t_0) ≤ 3 ms and variable seeing. In these conditions we observed a total of 20 targets, but we could only obtain good quality datasets for seven of them. They are included in Table 1. As shown in the table, some of the targets were even observed without AO owing to the unsuitable atmospheric conditions and poor LGS performance.

All the targets were observed with the S54 objective, providing a field of view of $54'' \times 54''$ and a nominal plate scale of $0''.054$. The data was obtained in one or several near-IR filters (*JHK_s*), depending on the atmospheric conditions and brightness. To estimate and remove the sky background, we observed the targets applying random offsets between the individual exposures (‘Autojitter’ mode).

The data was reduced using *eclipse* (Devillard 1997) and following the standard steps for near-IR imaging data: the images were dark-subtracted and flat-field-divided, and bad pixels were masked out. The sky background was estimated and subtracted from all the individual images. Finally, the frames were shifted and co-added to generate the final stacked image. Since the atmospheric conditions were variable during the observations, some of the individual frames showed a low image quality. To improve the final spatial resolution of the combined data, we removed the worst individual images, i.e. those with the lowest Strehl ratio and the largest FWHM, and kept only those with the best AO performance.

The observing log is given in Table 2. As can be seen, the seeing and coherence time were not optimal for AO+LGS observations, and this is reflected in the final FWHM and Strehl ratios measured on the combined images.

4. Results

Five of the seven BDs observed with NACO+LGS are apparently single. We estimated the sensitivity limit as a function of the separation for all of them (see Fig. 1) in the different NACO filters. The curves have been estimated from the point spread function (PSF) radial profiles of the targets, while computing the standard deviation of the noise in bins of 20 pixels and one pixel step. We derived the difference in magnitudes at a $3\text{-}\sigma$ level normalizing by the peak intensity of the PSF.

Usually, the best combination of sensitivity and angular resolution is achieved in the H band. To derive the sensitivity limits in this band, we used the *H* mag listed in Table 1. For the targets with MKO filter system photometry, we converted the magnitudes into the 2MASS system using the relations from Stephens & Leggett (2004). We obtain $H_{2\text{MASS}} \sim H_{\text{MKO}} - 0.04$ mag for the given spectral types. We reach $3\text{-}\sigma$ magnitude limits between $H \sim 19\text{-}21$ mag for separations of $0''.5$ (see Table 4). For an average distance of ~ 15 pc and ages of 1 Gyr and 5 Gyr, this magnitude interval corresponds to masses of $\sim 11\text{-}7 M_{\text{Jup}}$, and $\sim 30\text{-}18 M_{\text{Jup}}$, respectively, according to COND evolutionary tracks (Chabrier et al. 2000). For each individual target, we estimated the approximate spectral type (Sp. Type_{lim}) that corresponds to the *H*-band limiting magnitude ($3\text{-}\sigma$) using

² <http://www.eso.org/sci/facilities/paranal/instruments/naco/doc>

Table 1. Sample of observed brown dwarfs

Target	RA (J2000)	DEC (J2000)	Sp. Type	H^* (mag)	d (pc)	Reference
WISE J0612-3036	06 12 13.8	-30 36 12.2	T6	17.06±0.11	17.0	1
2MASS J1114-2618	11 14 51.3	-26 18 23.5	T7.5	15.73±0.12	10±2	2,3
WISE J1436-1814	14 36 02.2	-18 14 21.9	T8 pec	>17.62	16.8	1,4
WISE J1612-3420	16 12 15.9	-34 20 27.1	T6.5	16.96±0.03**	16.2	1,4
WISE J1959-3338	19 59 05.7	-33 38 33.7	T8	17.18±0.05**	11.6	1
WISE J2255-3118	22 55 40.7	-31 18 42.0	T8	17.70±0.11**	13.0	1
WISE J2327-2730	23 27 28.7	-27 30 56.5	L9	15.481±0.103	21.7	1

Notes: * 2MASS photometry except for ** with MKO filter system photometry; ¹ Kirkpatrick et al. (2011); ² Tinney et al. (2005); ³ Aberasturi et al. (2014); ⁴ Kirkpatrick et al. (2012)

Table 2. Observing log.

Date	Target	Filter	Exp. time (sec)	Seeing ¹ (arcsec)	t_0^1 (ms)	Airmass	LGS mode ²	FWHM ³ (arcsec)	Strehl ⁴ (%)
2012-09-08	WISE 0612-3036	<i>J</i>	300	0.8	2.5	1.1	non-AO	–	–
		<i>H</i>	180	0.7	2.5	1.3	<i>se</i>	–	–
		<i>K_s</i>	420	0.7	3.0	1.2	non-AO	–	–
	WISE 2255-3118	<i>H</i>	780	1.3	1.1	1.0	<i>se</i>	0.50	2.1
		<i>K_s</i>	840	1.0	1.5	1.0	<i>se</i>	0.40	3.3
		<i>H</i>	660	0.9	1.7	1.3	<i>se</i>	0.37	3.2
2013-05-19	2MASS J1114-2618	<i>J</i>	480	0.9	1.5	1.2	<i>tt</i>	0.40	1.8
		<i>H</i>	480	0.9	2.0	1.1	<i>tt</i>	0.22	4.8
		<i>K_s</i>	480	0.9	2.0	1.1	<i>tt</i>	0.14	11.0
	WISE 1959-3338	<i>J</i>	600	0.9	2.0	1.0	<i>tt</i>	0.39	2.7
		<i>H</i>	400	0.9	1.7	1.0	<i>tt</i>	0.27	5.0
		<i>K_s</i>	300	0.8	2.0	1.0	<i>tt</i>	0.25	8.0
2013-07-01	WISE 1436-1814	<i>H</i>	240	1.1	4.0	1.0	<i>se</i>	0.53	2.3
		<i>K_s</i>	240	1.1	4.0	1.0	<i>se</i>	0.29	4.6
	WISE 1612-3420	<i>H</i>	900	1.0	4.0	1.0	non-AO	0.41	2.4
		<i>K_s</i>	800	1.0	4.0	1.0	non-AO	0.30	4.0

Notes: ¹ Average values from the Differential Image Motion Monitor (DIMM); ² *se*: seeing enhancer, *tt*: tip-tilt (see text for details); ³ Full width at half maximum (FWHM) measured on the target; ⁴ Strehl ratio measured on the target, except in the case of WISE 0612-3036, which is resolved into a tight binary system.

Table 3. Contrast and sensitivity limits ($3\text{-}\sigma$) in the H -band at a separation of $0''.5$. The magnitudes are provided in the 2MASS system.

Target	ΔH (mag)	$H_{\text{lim}}@0.5''$ (mag)	Sp. type lim^1
2MASS 1114- 2618	4.7	20.4	Y0
WISE 1436-1814	2.0	>19.6	>T9
WISE 1612-3420	3.2	20.2	T9
WISE 1959-3338	3.5	20.7	Y0
WISE 2327-2730	3.7	19.2	T8

¹ Spectral type that corresponds to the limiting H -mag according to the M_H -Sp. Type relation from Kirkpatrick et al. (2012).

the M_H versus spectral type relation derived by Kirkpatrick et al. (2012), and the individual distances from Table 1. This value is included in the last column of Table 4. In the case of WISE 1114-2618, we achieve a ΔH value of 4.7 mag at $0''.5$. This is deeper than the HST/F164N observations presented by Aberasturi et al. (2014), with a contrast of 1.5 mag at a separation of $0''.6$.

4.1. WISE 0612-3036

We have resolved WISE 0612-3036 (WISE0612, hereafter) into a subarcsecond binary (Fig. 2). The two objects are detected in the three bands, JHK_s with an estimated separation of $\rho = 350 \pm 5$ mas and position angle of $\text{PA} = 235 \pm 1^\circ$. The values

are derived computing the average and standard deviation of the measurements in the three bands. We note that only the H -band data was obtained with LGS assisted AO, while the subsequent JK_s data was obtained in open loop owing to technical problems with the laser.

We performed PSF stellar photometry of the binary system with ALLSTAR in DAOPHOT II (Stetson 1992). For the photometry we used the final stacked images in each filter. The PSF was constructed using three or four stars in the field of view for the J and HK_s bands, respectively. The typical PSF errors of both components are in the range of 0.012–0.034 mag. For the transformation to the standard 2MASS JHK_s system, we used the only star in the field with 2MASS photometry: 2MASS J06121227-3036100 with $\alpha(2000) = 6^{\text{h}} 06^{\text{m}} 12^{\text{s}}.27$ and $\delta(2000) = -30^\circ 36' 10''.0$ and apparent magnitudes of $J = 15.915 \pm 0.080$ mag, $H = 15.141 \pm 0.066$ mag, and $K_s = 15.024 \pm 0.139$ mag. The final errors of the photometry are weighted means of the PSF errors and errors of the standard star. To double check the PSF photometric calibration with the bright star 2MASS J06121227-3036100, we estimated its K_s -band magnitude using a standard star observed at the end of the night. We find that the difference between the 2MASS tabulated value and our calibrated photometry is only 0.04 mag.

The estimated magnitudes for the two components in the 2MASS system are provided in Table 4. Kirkpatrick et al. (2011) report magnitudes of $J = 17.00 \pm 0.09$, $H = 17.06 \pm 0.11$, and $K_s = 17.34 \pm 0.21$ for the unresolved system. If we correct them for

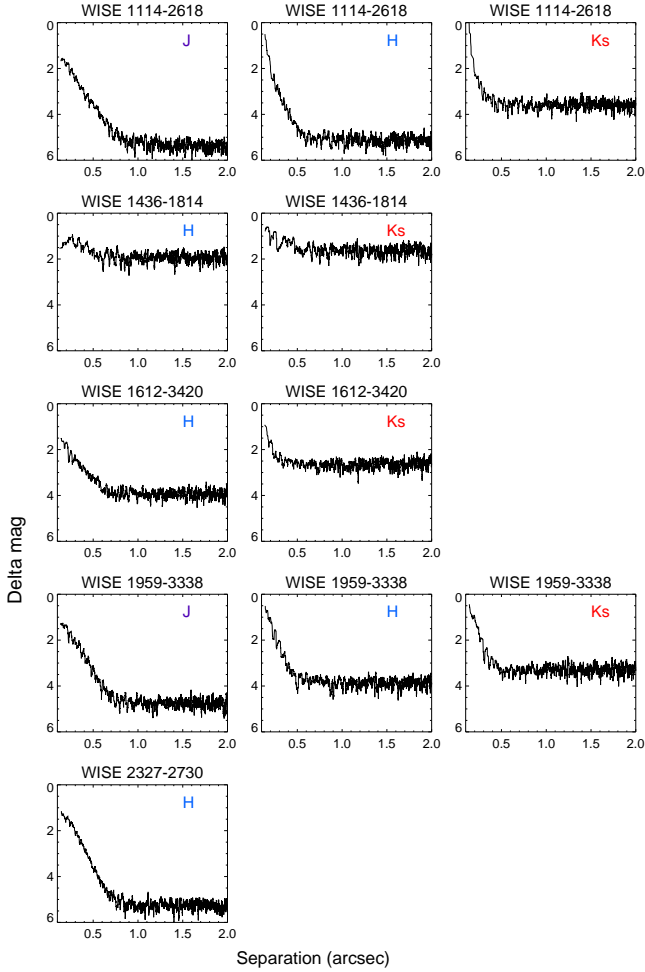


Fig. 1. Sensitivity limit of the NACO observations. We show the curves for the five apparently single sources, one target per row, in the different NACO filters. They were computed as the $3\text{-}\sigma$ standard deviation of the PSF radial profile.

binarity, the difference between our PSF photometry and these values are -0.12 , 0.14 , and 0.16 in JHK_s , respectively, which are consistent within the given uncertainties.

The primary (A) is the brightest object located to the NE (see Fig. 2). Kirkpatrick et al. (2011) classify the unresolved object as a T6 dwarf based on near-IR spectroscopy. The difference in magnitudes between the two components are $\Delta J = -0.05 \pm 0.14$ mag, $\Delta H = -0.10 \pm 0.14$ mag, and $\Delta K_s = -0.13 \pm 0.24$ mag, so we can assume similar spectral types for the two objects.

We have plotted the binary components in a near-IR color-color diagram (see Fig. 3) and compared them with well known T-type dwarfs from Dupuy & Liu (2012, Table 10) with available 2MASS photometry. We have only included objects with photometric uncertainties smaller than 0.2 mag in the three bands. The WISE0612 system falls within the region of the late-T dwarfs with a very blue $H - K_s$ color. As explained in Burgasser et al. (2002), this is expected in late-T dwarfs since the $2.1\mu\text{m}$ peak starts to flatten until it is suppressed for the latest type objects. This is indeed the case of WISE0612, which shows

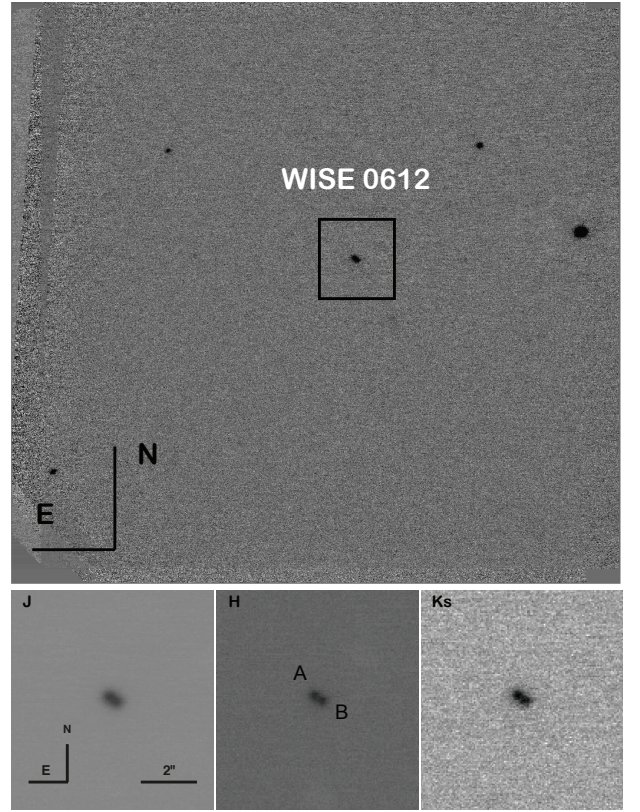


Fig. 2. NACO/LGS observations of WISE 0612-3036. The top panel shows the $\sim 54'' \times 54''$ NACO FOV. The target, WISE-0612-3036, is in the center of the black square. The star 2MASSJ06121227-3036100, used to calibrate the JHKs photometry of the binary system, is the brightest source in the west. The bottom panels show a zoom on the newly discovered binary in JHK_s .

Table 4. Properties of the binary system WISE 0612-3036 AB.

NACO photometry		
Parameter	WISE 0612A	WISE 0612B
J	17.85 ± 0.10	17.89 ± 0.10
H	17.62 ± 0.10	17.73 ± 0.10
K_s	18.18 ± 0.14	18.33 ± 0.20
$J - H$	0.25 ± 0.14	0.20 ± 0.14
$H - K_s$	-0.60 ± 0.17	-0.60 ± 0.22
$J - K_s$	-0.40 ± 0.17	-0.42 ± 0.22
Binary parameters		
ρ (mas)	350 ± 5	
ρ (au)	11 ± 2	
PA (deg)	235 ± 1	
Distance (pc)	31 ± 6	

no emission peak at $2.1\mu\text{m}$ in the near-IR spectrum obtained by Kirkpatrick et al. (2011).

The spectrophotometric distance to the unresolved source, based on its WISE W2 magnitude and its spectral type, is ~ 17 pc (Kirkpatrick et al. 2011). To derive the distance to the new binary system we have the mean 2MASS absolute magnitudes as a function of the spectral type from Dupuy & Liu (2012). The values derived for a T6 dwarf are $M_J = 15.35 \pm 0.02$, $M_H = 15.32 \pm 0.02$ mag, and $M_{K_s} = 15.68 \pm 0.01$ mag, with typical dispersions of 0.11 , 0.17 , and 0.33 mag, respectively. Using these values, we derived distances of $\sim 31 \pm 2$ pc (J -band),

29 ± 3 pc (H -band) and 32 ± 5 pc (K_s -band) and adopted an average value of $d = 31\pm 6$ pc for the rest of the paper.

Assuming that the two objects are bound, we represent the binary components in several color-absolute magnitude diagrams (see Fig. 4), together with a sample of MLT dwarfs with the measured parallaxes included in Dupuy & Liu (2012). We excluded objects with 2MASS photometric errors larger than 0.5 mag, and relative errors in their parallaxes ($\delta\pi/\pi$) larger than 0.6. As expected, the two binary components of WISE0612 lie in the region between T5-T7 dwarfs, with very blue $H - K_s$ and $J - K_s$ colors.

For the assumed distance of 31 ± 6 pc, the projected separation of the binary is $\rho \sim 11\pm 2$ au. Since the age of the system is unknown, we estimated the mass of the objects assuming two ages of ~ 1 Gyr and 5 Gyr. According to COND evolutionary tracks (2MASS system, Chabrier et al. 2000), we derived masses of $\sim 30 M_{\text{Jup}}$ (1 Gyr) and $\sim 60 M_{\text{Jup}}$ (5 Gyr) for the individual components. For a circular orbit, we derived orbital periods of ~ 150 yr for 1 Gyr and ~ 105 yr for 5 Gyr.

Finally, we note that a single-epoch observation is not enough to classify the binary as bound. Although additional data is needed to confirm it as a common proper motion pair, the small angular separation makes a random coincidence unlikely. We have estimated the probability of a background object lying close to the target using the number sources detected in the NACO H -band image. We detect eight sources in the $\sim 56'' \times 56''$ field of view. Since the companion candidate is detected at a separation of $0''.35$, the probability of detecting an object in an area of $\pi \times (0''.35)^2 = 0.3848$ arcsec² around the target is $8 \times (0.3848/56^2)$, that is, 0.09%. If we only consider the detected sources with a similar brightness to the companion (2), we derive a probability of 0.02%. We have also checked that there is no object at the given position in the Palomar Observatory Sky Survey (POSS) II images.

On the other hand, the proper motion of the primary estimated by Kirkpatrick et al. (2011) is $\mu_\alpha \cos \delta = -137\pm 22$ mas/yr and $\mu_\delta = -256\pm 21$ mas/yr, that is, $\sim 0.3''$ /yr. Therefore, the binary can be confirmed with second-epoch non-AO observations obtained after 3-4 yrs, to allow the BD enough time to move far enough from the companion, if it turns out that the latter is not co-moving.

4.2. WISE 2255-3118

In the case of the T8 dwarf WISE J2255-3118 (WISE2255, hereafter), the final image quality was not good enough to detect very close companions. However, we have detected a very faint source in the K_s band at a separation of $\sim 1''.3$ (see Fig. 5). This source is marginally detected in the H band. The estimated distance to the source, 13 pc (Kirkpatrick et al. 2011), implies a projected separation of ~ 17 au.

We performed aperture photometry on the HK_s -band images and calibrated it using standard stars observed during the night. We derive $H = 17.64\pm 0.18$ mag and $K_s = 17.47\pm 0.25$ mag for the primary. For the faint object we estimate $K_s = 20.5\pm 0.3$ mag and $H > 20.6$ mag and a color of $H - K_s \lesssim 0.1$ mag.

If bound, the companion candidate would be at a distance of 13 pc, which implies a $M_{K_s} \sim 19.9$ mag. When we compare its properties to those of the T dwarfs represented in the central lower panel of Fig. 4, we see that the object does not follow the sequence of the coldest T dwarfs, displaying a redder $H - K_s$ color. In this panel we also compared WISE2255 with WISE 1711+3500, a physical binary system with very similar properties: it consists of a T8 primary and a T9.5 companion

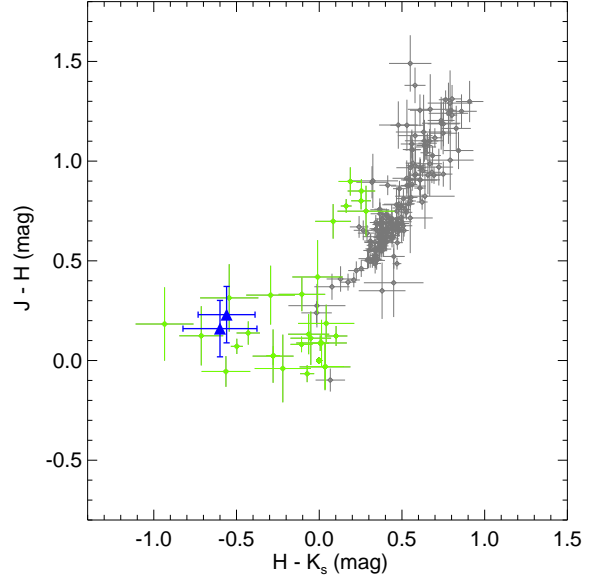


Fig. 3. Color-color near-IR diagram. We have included a sample of ultracool dwarfs from Dupuy & Liu (2012): the small gray diamonds represent M- and L-dwarfs, while the green diamonds are T dwarfs. We have only plotted objects with photometric uncertainties smaller or equal to 0.2 mag. The binary components of WISE0612 are represented by blue triangles.

with $\Delta K = 3$ mag (Liu et al. 2012). The difference in the H band between the two components is ΔH of -2.83 , and its $H - K_{s,\text{MKO}}$ color is -0.42 ± 0.17 . Using the relations by Stephens & Leggett (2004) for a T9 dwarf (the coldest object in their sample), we can convert its magnitudes into the 2MASS system ($K_{s,2\text{MASS}} = K_{s,\text{MKO}} + 0.16$, and $H_{2\text{MASS}} = H_{\text{MKO}} + 0.04$), obtaining $H - K_{s,2\text{MASS}} = -0.54$, significantly bluer than the upper limit reported for the WISE2255 companion candidate.

Finally, we also compared the photometry of the companion candidate with five Y dwarfs included in Liu et al. (2012) and Leggett et al. (2013). Since they all have HK_s photometry in the MKO system, we have converted them to the 2MASS system following the same procedure described above. The result is displayed in Fig. 4 (low central panel). The companion is redder than the Y dwarfs, but it lies close enough to their locus, preventing us from drawing a firm conclusion about the nature of this object.

We searched in public archives for additional data on this source and found *HST*/WFC3 data obtained in two near-IR filters, F110W and F160W (Program 12972, P.I. Gelino). The observations were obtained on 2012 October 17 in MULTIACCUM mode and following a four dithering pattern. The total exposure time was ~ 1200 sec in the two filters. We retrieved the final calibrated images (*flt* name extension) from the Hubble Legacy Archive (HLA) and reprocessed them using the routines within the DrizzlePac³ package. In particular, we used MULTIDRIZZLE to combine the exposures into a master image, resampling onto a finer pixel scale and correcting for geometric distortions in the camera. (We selected a final_scale of 0.09 ''/pixel and final_pixfrac of 0.8.) The T dwarf and the companion are clearly detected in the final *HST* images (see Fig. 6), and the analysis of the two images with SEXTRACTOR (Bertin & Arnouts

³ <http://drizzlepac.stsci.edu/>

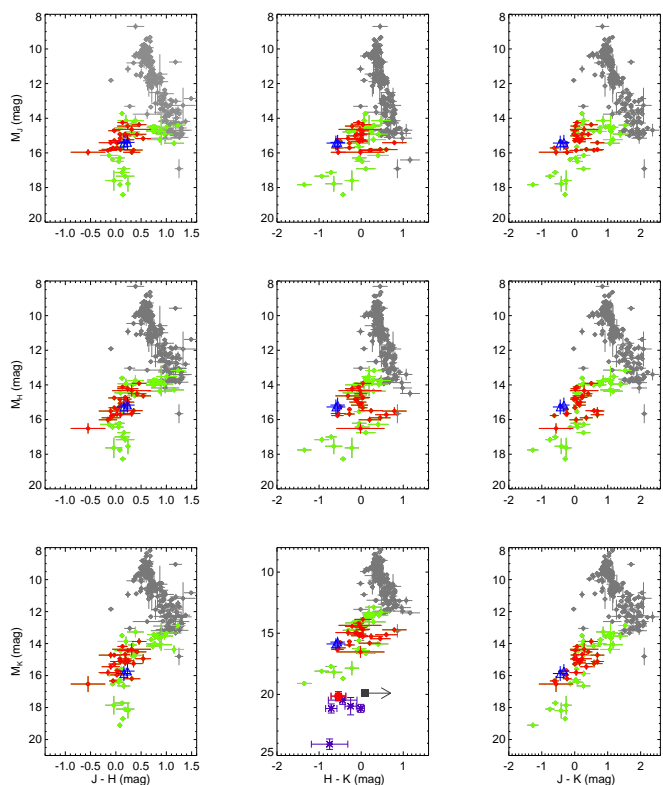


Fig. 4. Near-IR color-magnitude diagrams. We represent a sample of ultracool dwarfs with measured parallaxes and 2MASS photometry from Dupuy & Liu (2012): gray diamonds represent ML-dwarfs and green diamonds the T dwarfs. We have highlighted in red the T-dwarfs with spectral types between T5 and T7. The binary components of WISE0612 are represented by blue open triangles. In the lower central panel, the faint companion candidate to WISE2255 is represented by a filled square and WISE 1711+3500B (T9.5, Liu et al. 2012) by a filled circle. A sample of 4 Y-dwarfs (Liu et al. 2012; Leggett et al. 2013) are indicated by asterisks.

1996) and PSFEx (Bertin 2011) reveals that the faint companion candidate is an extended source. To visualize it, we represented the HST PSF-subtracted images in Figure 6, where the companion shows strong residuals in comparison to the T dwarf. This is consistent with the concentration index (CI) derived by the *HST* team and included in the HLA SEXTRACTOR catalog for the F160W band (Data Release 8). This index is defined as the difference in magnitude from two different apertures ($0''.09$ and $0''.27$), and it is used to separate extended from point-like sources. They measure a $CI = 1.4$ for the companion candidate, while point-like sources in the WFC3 show $0.5 < CI < 1.0$. We note that the *HST* image is relatively crowded, with a large number of spatially resolved galaxies. In fact, the HLA catalog contains 275 detected sources, with 235 displaying $CI > 1.0$.

An extended source is consistent with a background galaxy or with a binary. In the latter case, and if bound to the primary, the binary components would be cooler than T8, and probably in the Y-dwarf regime. However, with the current data we cannot distinguish between the two scenarios.

That the detected source is extended, together with the red $H - K_s$ color, suggests that the faint object is most probably a background galaxy, although additional imaging is needed to test whether the objects are co-moving or not.

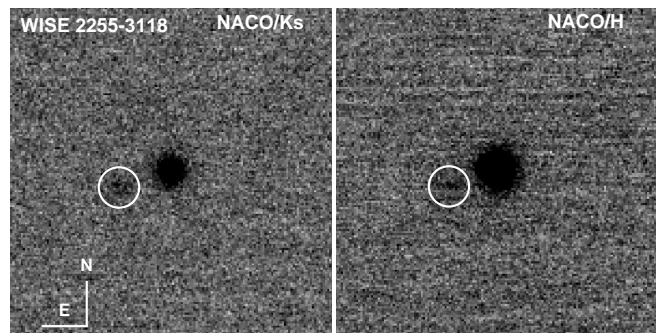


Fig. 5. NACO/LGS K_s & H observations of WISE 2255-3118. We display a field of $8'' \times 8''$. A faint source (encircled) is detected at $\sim 1''.3$ SE from the T dwarf.

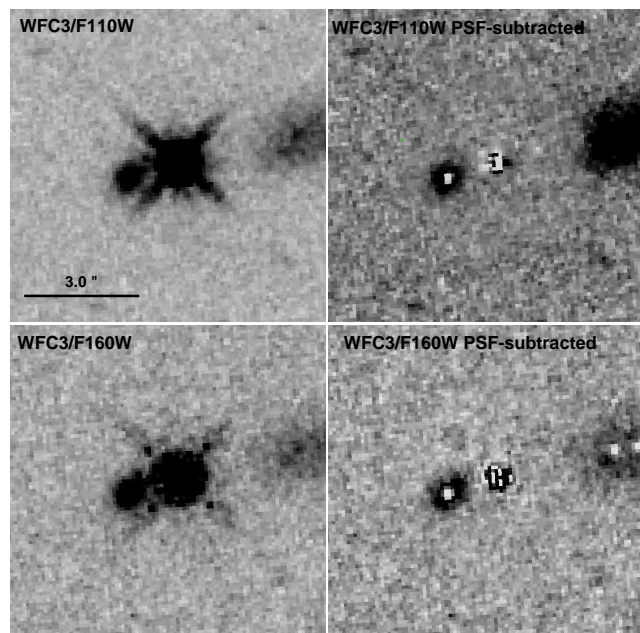


Fig. 6. HST/WFC3 F110W and F160W reduced images of WISE 2255-3118. We display a field of $8'' \times 8''$. North is up and east to the left. The companion candidate is clearly resolved in the two filters. The PSF-subtracted images are displayed on the right panels, where the companion candidate shows large residuals consistent with an extended source.

4.3. Comparison with T-dwarf binaries

To put our study into context, we compared the properties of WISE 0612-3036 with other T-dwarf binaries from different AO and HST studies (see Table 5). We have represented the spectral types of the secondaries versus the spectral types of the primaries in Figure 7. Their projected separation in the sky (in au) have been color-coded. As seen in Figure 7, all the early-T primaries ($SpT < T2$) have secondaries later than T5, while most of the late-T primaries ($SpT \geq T4$) show nearly equal mass companions (typical errors in spectral typing are between 0.5-1 type). Among the latter group, the separations range between 2-15 au, with only three binaries showing separations larger than or equal to 8 au. WISE 0612-3036 is among these three binaries with a projected separation of 11 au.

Table 5. Summary of known T-dwarf binary systems

Name	SpT A	SpT B	Distance [pc]	ρ [mas]	ρ [au]	Reference
SDSS 102109.69-030420.1	T1	T4	29 \pm 4	172 \pm 5	5.0 \pm 0.7	Burgasser et al. (2006)
2MASS J14044941-3159329	T1	T5	\sim 23	133.6 \pm 0.6	\sim 3.1	Looper et al. (2008)
ϵ Indi B	T1	T6	3.626 \pm 0.013	732 \pm 2	2.654 \pm 0.012	McCaughrean et al. (2004)
SDSS 153417.05+161546.1	T1.5	T5.5	\sim 36	110 \pm 5	\sim 4	Liu et al. (2006)
SDSS 092615.38+584720.9	T4	T4	38 \pm 7	70 \pm 6	2.6 \pm 0.5	Burgasser et al. (2006)
WISEPA 184124.73+700038.0	T5	T5	40.2 \pm 4.9	70 \pm 14	2.8 \pm 0.7	Gelino et al. (2011)
2MASS J15344984-2952274	T5	T5.5	16 \pm 5	140.3 \pm 0.57	2.3 \pm 0.5	Burgasser et al. (2003); Liu et al. (2008)
2MASS J12255432-2739466	T6	T8	11.2 \pm 0.5	282 \pm 5	3.17 \pm 0.14	Burgasser et al. (2003)
2MASS J15530228+1532369	T6.5	T7	12 \pm 2	349 \pm 5	4.2 \pm 0.7	Burgasser et al. (2006)
WISEPA J171104.60+35000036.8	T8	T9.5	19 \pm 3	780 \pm 2	15.0 \pm 2.0	Liu et al. (2012)
WISEPA J045853.90+643452.6	T8.5	T9	10.5 \pm 1.4	510 \pm 20	5.0 \pm 0.4	Gelino et al. (2011)
WISE J014656.66+423410.0	T9	Y0	10.6 \pm 1.5	87.5 \pm 2.0	0.93 \pm 0.14	Dupuy et al. (2015)
WISEPC J121756.91+162640.2	T9	Y0	10.5 \pm 1.7	759.2 \pm 3.3	8.0 \pm 1.3	Liu et al. (2012)
CFBDSIR J1458+1013	T9.5	T10	23.1 \pm 2.4	110 \pm 5	2.6 \pm 0.3	Liu et al. (2011)

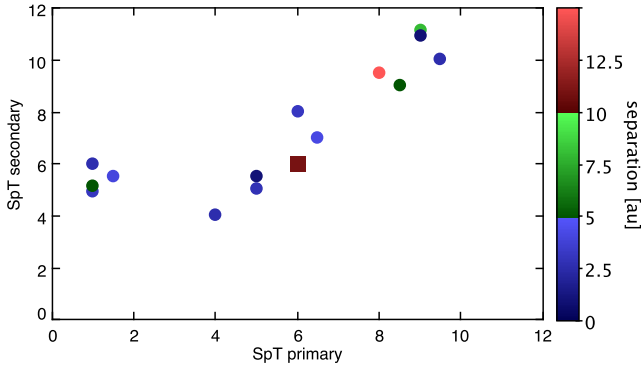


Fig. 7. Known T-dwarf binaries. We have represented the spectral types of the secondaries versus the primaries for known T-dwarf binaries (circles). 0 stands for T0, 10 for T10, and 11 for Y0. The color code is related with the projected separation (in au) of the binaries. Most of them show separations smaller than 5 au, while only three show $\rho \approx 8$ au. WISE 0612-3036 (filled square) is among these three wide binaries with a projected separation of 11 au.

5. Conclusions

We have observed seven BDs with the NACO+LGS system to look for close companions. In general, the observing conditions were not optimal for the LGS, resulting in poor corrections that did not allow the innermost regions around the targets to be explored.

Our main findings can be summarized as follows:

- Five targets are apparently single with 3- σ limiting magnitudes of H between 19–21 mag at 0".5.
- The T-dwarf WISE 0612-3036 is clearly resolved into a sub-second binary. PSF-photometry of the binary has allowed us to derive the individual JHK_s magnitudes of the two components, which are consistent with a very similar spectral type of T6. Using absolute magnitude-spectral type relationships in JHK_s , we estimate a distance to the binary of $d \sim 31 \pm 6$ pc, which implies a projected separation of $\rho = 11 \pm 2$ au. Additional observations are needed to confirm the system as bound.
- The target WISE 2255-3031 shows a very faint source at a separation of 1".3 SE from the primary. Its $H - K_s$ color (> 0.1 mag) is redder than the colors of the latest T dwarfs

and Y dwarfs. Since *HST* public archival data in two near-IR filters shows that the source is extended, we suggest that it is most probably a background galaxy.

- Similar to other known late T-dwarf binaries, WISE 0612-3036 is comprised of two nearly equal-mass objects. Its projected separation, 11 au, is larger than the average value for these binaries (~ 5 au).

Acknowledgements. We thank the referee, C. Reyle, for her useful comments. This research has been funded by Spanish grants AYA2010-21161-C02-02 and AYA2012-38897-C02-01. Support for NH, JB, RK, and DM is provided by the Ministry of Economy, Development, and Tourism's Millennium Science Initiative through grant IC120009, awarded to The Millennium Institute of Astrophysics, MAS. JB is supported by FONDECYT No.1120601, RK is supported by Fondecyt Reg. No. 1130140. DM is also supported by FONDECYT No.1130196 and by the Center for Astrophysics and Associated Technologies CATA PFB-06. CC acknowledges the support from project CONICYT FONDECYT Postdoctorado 3140592. We are indebted to the Paranal staff for their support during the runs. NH thanks H. Bouy for useful discussions. This research has benefited from the M, L, T, and Y dwarf compendium housed at DwarfArchives.org.

References

- Aberasturi, M., Burgasser, A. J., Mora, A., et al. 2014, *AJ*, 148, 129
- Albert, L., Artigau, É., Delorme, P., et al. 2011, *AJ*, 141, 203
- Bertin, E. 2011, in *Astronomical Society of the Pacific Conference Series*, Vol. 442, *Astronomical Data Analysis Software and Systems XX*, ed. I. N. Evans, A. Accomazzi, D. J. Mink, & A. H. Rots, 435
- Bertin, E. & Arnouts, S. 1996, *A&AS*, 117, 393
- Bouy, H., Brandner, W., Martín, E. L., et al. 2003, *AJ*, 126, 1526
- Bouy, H., Martín, E. L., Brandner, W., et al. 2008, *A&A*, 481, 757
- Burgasser, A. J., Kirkpatrick, J. D., Brown, M. E., et al. 2002, *ApJ*, 564, 421
- Burgasser, A. J., Kirkpatrick, J. D., Cruz, K. L., et al. 2006, *ApJS*, 166, 585
- Burgasser, A. J., Kirkpatrick, J. D., Reid, I. N., et al. 2003, *ApJ*, 586, 512
- Burningham, B., Pinfield, D. J., Lucas, P. W., et al. 2010, *MNRAS*, 406, 1885
- Chabrier, G., Baraffe, I., Allard, F., & Hauschildt, P. 2000, *ApJ*, 542, 464
- Cushing, M. C., Kirkpatrick, J. D., Gelino, C. R., et al. 2011, *ApJ*, 743, 50
- Delorme, P., Willott, C. J., Forveille, T., et al. 2008, *A&A*, 484, 469
- Devillard, N. 1997, *The Messenger*, 87, 19
- Dupuy, T. J. & Liu, M. C. 2012, *ApJS*, 201, 19
- Dupuy, T. J., Liu, M. C., & Leggett, S. K. 2015, *ArXiv e-prints*
- Epchtein, N., de Batz, B., Capoani, L., et al. 1997, *The Messenger*, 87, 27
- Gelino, C. R., Kirkpatrick, J. D., Cushing, M. C., et al. 2011, *AJ*, 142, 57
- Girard, J. H. V., Kasper, M., Quanz, S. P., et al. 2010, in *Society of Photo-Optical Instrumentation Engineers (SPIE) Conference Series*, Vol. 7736, *Society of Photo-Optical Instrumentation Engineers (SPIE) Conference Series*, 2
- Gizis, J. E., Burgasser, A. J., Faherty, J. K., Castro, P. J., & Shara, M. M. 2011, *AJ*, 142, 171
- Kirkpatrick, J. D., Cushing, M. C., Gelino, C. R., et al. 2011, *ApJS*, 197, 19
- Kirkpatrick, J. D., Gelino, C. R., Cushing, M. C., et al. 2012, *ApJ*, 753, 156
- Lawrence, A., Warren, S. J., Almaini, O., et al. 2007, *MNRAS*, 379, 1599
- Leggett, S. K., Morley, C. V., Marley, M. S., et al. 2013, *ApJ*, 763, 130
- Lenzen, R., Hartung, M., Brandner, W., et al. 2003, in *Society of Photo-Optical Instrumentation Engineers (SPIE) Conference Series*, Vol. 4841, *Instrument*

- Design and Performance for Optical/Infrared Ground-based Telescopes, ed. M. Iye & A. F. M. Moorwood, 944–952
- Liu, M. C., Delorme, P., Dupuy, T. J., et al. 2011, *ApJ*, 740, 108
- Liu, M. C., Dupuy, T. J., Bowler, B. P., Leggett, S. K., & Best, W. M. J. 2012, *ApJ*, 758, 57
- Liu, M. C., Dupuy, T. J., & Ireland, M. J. 2008, *ApJ*, 689, 436
- Liu, M. C., Leggett, S. K., Golimowski, D. A., et al. 2006, *ApJ*, 647, 1393
- Looper, D. L., Gelino, C. R., Burgasser, A. J., & Kirkpatrick, J. D. 2008, *ApJ*, 685, 1183
- McCaughrean, M. J., Close, L. M., Scholz, R.-D., et al. 2004, *A&A*, 413, 1029
- Pinfield, D. J., Gomes, J., Day-Jones, A. C., et al. 2014a, *MNRAS*, 437, 1009
- Pinfield, D. J., Gromadzki, M., Leggett, S. K., et al. 2014b, *MNRAS*, 444, 1931
- Rousset, G., Lacombe, F., Puget, P., et al. 2003, in *Society of Photo-Optical Instrumentation Engineers (SPIE) Conference Series*, Vol. 4839, *Adaptive Optical System Technologies II*, ed. P. L. Wizinowich & D. Bonaccini, 140–149
- Skrutskie, M. F., Cutri, R. M., Stiening, R., et al. 2006, *AJ*, 131, 1163
- Stephens, D. C. & Leggett, S. K. 2004, *PASP*, 116, 9
- Stetson, P. B. 1992, in *Astronomical Society of the Pacific Conference Series*, Vol. 25, *Astronomical Data Analysis Software and Systems I*, ed. D. M. Worrall, C. Biemesderfer, & J. Barnes, 297
- Tinney, C. G., Burgasser, A. J., Kirkpatrick, J. D., & McElwain, M. W. 2005, *AJ*, 130, 2326
- Tinney, C. G., Faherty, J. K., Kirkpatrick, J. D., et al. 2012, *ApJ*, 759, 60
- Wright, E. L., Eisenhardt, P. R. M., Mainzer, A. K., et al. 2010, *AJ*, 140, 1868